Multiple-scattering theory of electron transport in disordered metals in the muffin-tin potential model. I. Effective-medium approximation formulation and the separation of off-shell corrections

1989 J. Phys.: Condens. Matter 1 6381

(http://iopscience.iop.org/0953-8984/1/36/006)

J. Phys.: Condens. Matter 1 (1989) 6381–6393. Printed in the UK

Multiple-scattering theory of electron transport in disordered metals in the muffin-tin potential model: I. Effective-medium approximation formulation and the separation of off-shell corrections

M Itoh†, H Beck‡ and R Frésard‡

† Department of Physics, Faculty of Science, Shimane University, Matsue 690, Shimane, Japan

‡ Institut de Physique, University of Neuchatel, Rue A-L Breguet 1, CH-2000, Neuchatel, Switzerland

Received 1 December 1988

Abstract. The effective-medium approximation formulation of electron transport in disordered metals due to Roth and Singh is reconsidered using the muffin-tin potential model. The theory is reduced into a tractable form by using the non-overlapping condition of muffin-tin spheres. The major part of the off-shell correction is shown to be absorbed in the on-shell expression by adding simple correction factors.

1. Introduction

The description of electron transport in terms of the T-matrix in disordered metals has been an attractive problem for quite a long time because of its simplicity in describing the scattering event from individual scattering centres. The non-overlapping muffin-tin potential model is expected to be especially suitable considering the success of the KKR-Z formalism in the electronic structure calculations. In particular the electronic density of states in this model is shown to be determined solely by the phase shifts of the scatterers in their arbitrary arrangement (Lloyd 1967). The model is therefore also useful for disordered materials, combined with analytic theories to deal with the randomness and the short-range order in the system. The coherent potential approximation has been applied to many solid alloys (see, for a review, Ehrenreich and Schwartz (1976)), and the calculations have also been performed for liquid metals using the effective-medium approximation (EMA) (Asano and Yonezawa 1980, Huisman *et al* 1981, Nishikawa and Niizeki 1984). The simplest application of the T-matrix formalism to electron transport is the so-called extended Ziman formula (Evans *et al* 1971). In spite of the fact that the formula neglects the multiple-scattering processes, it has been extensively used for liquid and amorphous metals including transition metals and rare earths. In these systems the multiple-scattering processes play essential roles and therefore a proper theoretical treatment must be developed to include higher-order scattering. The calculation using the Kubo–Greenwood formula and the Green function technique is the first candidate for this purpose. When it is combined with the T-matrix via the relation $G = G_0 + G_0TG_0$, however, the free-electron divergence in the conductivity is separated out. Therefore it

0953-8984/89/366381 + 13 $02.50

is not easy to obtain finite and physically meaningful results by summing higher-order contributions; one needs highly sophisticated renormalisation of the current vertex part as well as of the electron propagator. The second problem to be considered is that the ensemble average is to be carried out in a consistent way with the condition of a non-overlapping arrangement of the muffin-tin potentials. The problem has already become important in electronic structure calculations. The atomic short-range order must be taken into account properly for liquid and amorphous materials to avoid unphysical configurations. Finally it must be noted that the transport theory cannot be formulated in an on-shell form; that is, the phase shifts are not the only parameters which determine the transport property of the system. In this respect the situation is more difficult than in the calculation of the electronic density of states. Although information about the energy eigenvalues is included in the wavefunction outside the muffin-tin spheres, it is obvious that the whole wavefunction is necessary to calculate the current matrix element. In other words the acceleration of an electron inside the muffin-tin potential is related to the conduction.

In spite of the difficulties mentioned above, the scenario was almost completed by Roth and Singh (1982), who applied the EMA to transport. The EMA is known to be consistent with the non-overlapping condition (Roth 1975, Watabe and Yonezawa 1975, Yonezawa *et al* 1975, Yonezawa and Watabe 1975) and they obtained a set of coupled non-linear integral equations for the vertex corrections in terms of suitably renormalised quantities. However, these equations are apparently very complicated because of the electron momentum integrations in addition to the ionic momentum integrations, which is the reflection of the off-shell character of the problem. Their comment is that the calculations are just 'horrendous'.

In this paper, we diagrammatically analyse the theory to show that it is indeed possible to reduce the formalism into a tractable form. The integrations with respect to the electron momentum variables are in fact carried out if we deal with non-overlapping muffin-tin potentials. Then we separate the off-shell contributions into two parts. The major contribution is included in the 'conventional' terms which leads to the classical Boltzmann expression in the weak-scattering limit. The remaining small corrections can be neglected quantitatively and have no classical counterparts. We present the result in the angular momentum representation, which is not given explicitly in the paper by Roth and Singh.

2. EMA for the transport

We briefly review the transport theory by EMA for a muffin-tin potential model and rederive the result of Roth and Singh in a slightly different form, emphasising the role of the non-overlapping condition. We partly follow the notation due to Roth (1980). Given a T-matrix t_R associated with the muffin-tin potential located at $\boldsymbol{R}$, the EMA equations are written in the following form:

$$Q(\boldsymbol{R},\boldsymbol{R}') = Q_{\mathrm{d}}(\boldsymbol{R})\delta(\boldsymbol{R}-\boldsymbol{R}') + \int \mathrm{d}\boldsymbol{R}_1\, \tilde{G}(\boldsymbol{R},\boldsymbol{R}_1)Q(\boldsymbol{R}_1,\boldsymbol{R}') \tag{2.1}$$

$$\tilde{G}(\boldsymbol{R},\boldsymbol{R}') = G_0 g(\boldsymbol{R}-\boldsymbol{R}') + h(\boldsymbol{R}-\boldsymbol{R}') \int\int \mathrm{d}\boldsymbol{R}_1\, \mathrm{d}\boldsymbol{R}_2\, \tilde{G}(\boldsymbol{R},\boldsymbol{R}_1)Q(\boldsymbol{R}_1,\boldsymbol{R}_2)\tilde{G}(\boldsymbol{R}_2,\boldsymbol{R}') \tag{2.2}$$

$$Q_{\mathrm{d}}(\boldsymbol{R}) = t_R + t_R \eta(\boldsymbol{R}) Q_{\mathrm{d}}(\boldsymbol{R}) \tag{2.3}$$

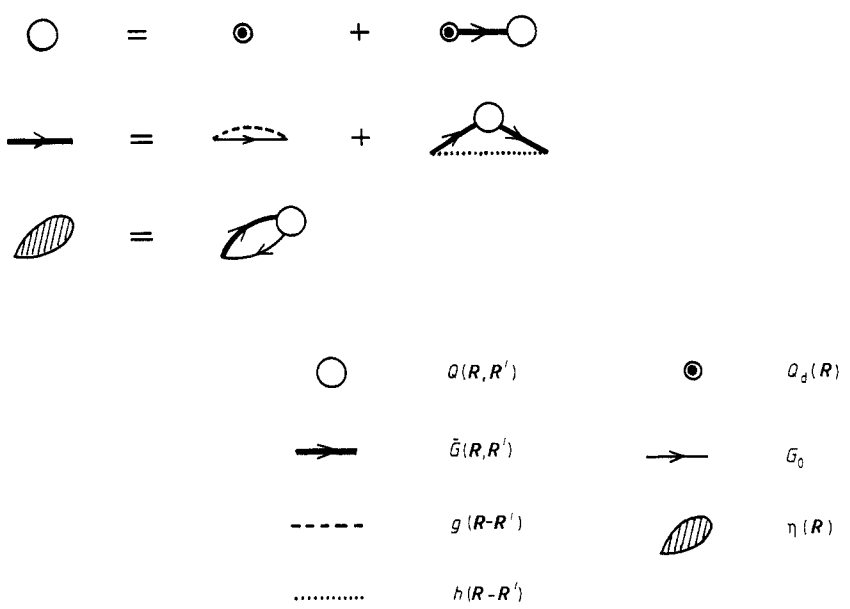

Figure 1. Diagrammatic representations of equations (2.1), (2.2) and (2.4). The topological equivalence to the tight-binding EMA should be noted.

$$\eta(\boldsymbol{R}) = \int\int \mathrm{d}\boldsymbol{R}_1\, \mathrm{d}\boldsymbol{R}_2\, \tilde{G}(\boldsymbol{R}, \boldsymbol{R}_1) Q(\boldsymbol{R}_1, \boldsymbol{R}_2) G_0. \tag{2.4}$$

In the above equations, G_0 is the free-electron propagator, $g(\boldsymbol{R} - \boldsymbol{R}')$ is the radial distribution function and $h(\boldsymbol{R}) = g(\boldsymbol{R}) - 1$. All the quantities are ensemble-averaged quantum operators for an electron dependent on parameters $\boldsymbol{R}, \boldsymbol{R}', \ldots$, representing the ionic positions. In particular, $Q(\boldsymbol{R}, \boldsymbol{R}')$, the scattering path operator, represents the scattering process starting from the position $\boldsymbol{R}$ and ending at $\boldsymbol{R}'$, and the T-matrix of the whole system is the sum of all the possible processes:

$$T = \int \mathrm{d}\boldsymbol{R}\, \mathrm{d}\boldsymbol{R}'\, Q(\boldsymbol{R}, \boldsymbol{R}'). \tag{2.5}$$

$Q_\mathrm{d}(\boldsymbol{R})$ is the operator representing only diagonal processes in Q, and $\eta(\boldsymbol{R})$ and $\tilde{G}(\boldsymbol{R}, \boldsymbol{R}')$ are the auxiliary quantities to complete the set of 'building blocks' of the theory. The diagrammatic representations of (2.1), (2.2) and (2.4) are given in figure 1. We see that the topological structure of $\eta(\boldsymbol{R})$ and $\tilde{G}(\boldsymbol{R}, \boldsymbol{R}')$ are equivalent, respectively, to those of the self-energy and the renormalised transfer in the tight-binding EMA (Roth 1975, Yonezawa and Watabe 1975). Our set of equations (2.1)–(2.4) are given in a slightly different form from that given by other researchers but the equivalence is clear. Now according to the Kubo–Greenwood formula the calculation of the conductivity tensor is reduced to that of

$$\Xi(E, E') = \mathrm{Tr}(\boldsymbol{J}\langle \hat{G} \boldsymbol{J} \hat{G}' \rangle), \tag{2.6}$$

where $\hat{G} = (E - \hat{H})^{-1}$ is the Green function operator for any given configuration and $\langle \ldots \rangle$ denotes the ensemble average. It should be noted that $\hat{G}$ is distinguished from $G \equiv \langle \hat{G} \rangle$; the circumflex is put on the operator before the ensemble average. We do not need it on $\boldsymbol{J}$ because $\hat{\boldsymbol{J}} = \boldsymbol{J}$ (the same can be said for G_0). The prime on the second $\hat{G}$ means that the energy has a different value $E' \neq E$, i.e. $\hat{G}' = (E' - \hat{H})^{-1}$. We follow

this convention hereafter. The quantity (2.6) is generally divided into a correlated and an uncorrelated part:

$$\Xi(E, E') = \Xi_0(E, E') + \Xi_c(E, E') \tag{2.7}$$

where

$$\Xi_0(E, E') \equiv \mathrm{Tr}(JGJG') \tag{2.8}$$

and $\Xi_c(E, E')$ is referred to as the vertex correction.

Roth and Singh gave a prescription for calculating the 'variation' in G, which is defined by

$$\delta G \equiv \langle \hat{G} J G' \rangle \tag{2.9}$$

and applied it to the EMA to calculate $\Xi(E, E')$. Here we repeat their argument in a slightly different form. First we take the variation in basic quantities. The variation in Q is derived from (2.1) and (2.3) by noting that $\delta t_R = t_R\, \delta G_0\, t_R$:

$$\delta Q(\boldsymbol{R}, \boldsymbol{R}') = \int \mathrm{d}\boldsymbol{R}_1\, Q(\boldsymbol{R}, \boldsymbol{R}_1)[\delta G_0 + \delta\eta(\boldsymbol{R}_1)]Q'(\boldsymbol{R}_1, \boldsymbol{R}') + \int\int \mathrm{d}\boldsymbol{R}_1\, \mathrm{d}\boldsymbol{R}_2\, Q(\boldsymbol{R}, \boldsymbol{R}_1)\delta\tilde{G}(\boldsymbol{R}_1, \boldsymbol{R}_2)Q'(\boldsymbol{R}_2, \boldsymbol{R}') \tag{2.10}$$

where $\delta G_0 \equiv G_0 J G_0'$. As for $\delta\tilde{G}$ and $\delta\eta$ we obtain, from (2.2) and (2.4),

$$\delta\tilde{G}(\boldsymbol{R}, \boldsymbol{R}') = \delta G_0\, g(\boldsymbol{R} - \boldsymbol{R}') + h(\boldsymbol{R} - \boldsymbol{R}') \int\int \mathrm{d}\boldsymbol{R}_1\, \mathrm{d}\boldsymbol{R}_2\, [\delta\tilde{G}(\boldsymbol{R}, \boldsymbol{R}_1) \times Q'(\boldsymbol{R}_1, \boldsymbol{R}_2)\tilde{G}'(\boldsymbol{R}_2, \boldsymbol{R}') + \tilde{G}(\boldsymbol{R}, \boldsymbol{R}_1)\delta Q(\boldsymbol{R}_1, \boldsymbol{R}_2)\tilde{G}'(\boldsymbol{R}_2, \boldsymbol{R}') + \tilde{G}(\boldsymbol{R}, \boldsymbol{R}_1)Q(\boldsymbol{R}_1, \boldsymbol{R}_2)\delta\tilde{G}(\boldsymbol{R}_2, \boldsymbol{R}')] \tag{2.11}$$

$$\delta\eta(\boldsymbol{R}) = \int\int \mathrm{d}\boldsymbol{R}_1\, \mathrm{d}\boldsymbol{R}_2\, [\delta\tilde{G}(\boldsymbol{R}, \boldsymbol{R}_1)Q'(\boldsymbol{R}_1, \boldsymbol{R}_2)G_0' + \tilde{G}(\boldsymbol{R}, \boldsymbol{R}_1)\delta Q(\boldsymbol{R}_1, \boldsymbol{R}_2)G_0' + \tilde{G}(\boldsymbol{R}, \boldsymbol{R}_1)Q(\boldsymbol{R}_1, \boldsymbol{R}_2)\delta G_0']. \tag{2.12}$$

Finally the variation in G is performed using $G = G_0 + G_0 T G_0$;

$$\delta G = GJG' + G_0(\delta T - T\,\delta G_0\, T')G_0' \tag{2.13}$$

and therefore it becomes, from (2.5), (2.7) and (2.8),

$$\Xi_c(E, E') = \int\int \mathrm{d}\boldsymbol{R}_1\, \mathrm{d}\boldsymbol{R}_2 \int\int \mathrm{d}\boldsymbol{R}_3\, \mathrm{d}\boldsymbol{R}_4\, \mathrm{Tr}\{\delta G_0\, Q(\boldsymbol{R}_1, \boldsymbol{R}_2) \times [\delta\tilde{G}(\boldsymbol{R}_2, \boldsymbol{R}_3) - \delta G_0]Q'(\boldsymbol{R}_3, \boldsymbol{R}_4)\} + \int\int\int \mathrm{d}\boldsymbol{R}_1\, \mathrm{d}\boldsymbol{R}_2\, \mathrm{d}\boldsymbol{R}_3\, \mathrm{Tr}\{\delta G_0\, Q(\boldsymbol{R}_1, \boldsymbol{R}_2) \times [\delta G_0 + \delta\eta(\boldsymbol{R}_2)]Q'(\boldsymbol{R}_2, \boldsymbol{R}_3)\} \tag{2.14}$$

where we have made use of the relation $G_0' J G_0 = G_0 J G_0' = \delta G_0$.

Equations (2.11), (2.12) and (2.14) are expressed diagrammatically in figure 2. Note that the uncorrelated part is included in the contribution from $\tilde{G}$ in (2.14) and should be subtracted. The diagram (II) in figure 2(*C*) refers to this correction. Equations (2.10)–(2.12) are to be solved simultaneously to obtain $\delta\tilde{G}$ and $\delta\eta$. The first and the second

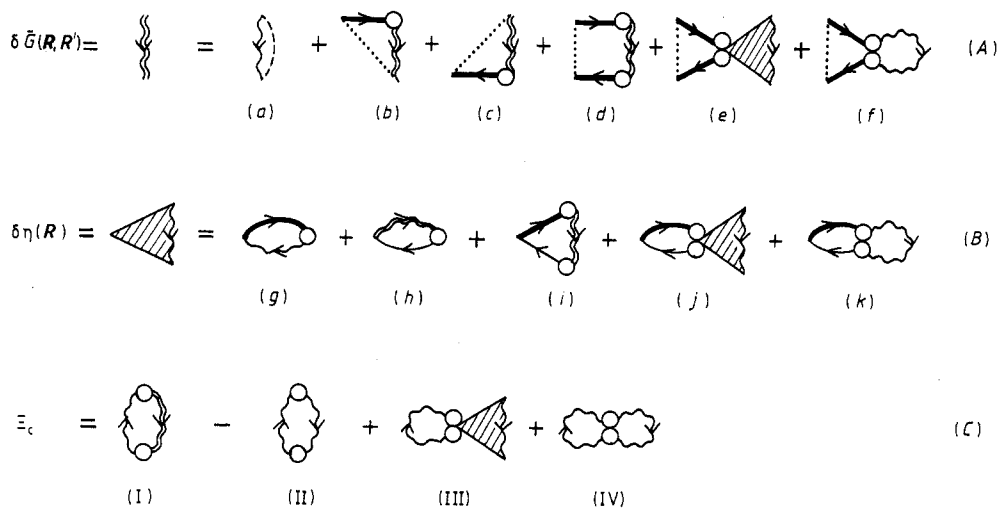

Figure 2. Diagrammatic representations of equations (2.11), (2.12) and (1.14). Topological equivalence to the result of Itoh *et al* (1981) is clearly seen.

terms of (2.14) correspond respectively to the contributions from δW and δK_0 in the paper by Roth and Singh. Our equations appear to be different from their equations; the diagonal part is particularly different. This is because our starting equations are written in different forms. The present form is more convenient for later development because it has exactly the same topological structure as the EMA transport theory in the tight-binding representation developed by Itoh *et al* (1981).

3. Angular momentum representation and off-shell corrections

So far we have developed the formalism in the general operator form. The trace operation to calculate the conductivity tensor may be performed in an arbitrary representation. However, since our muffin-tin potential is spherical, the decomposition of the electron wave into its angular momentum components is particularly useful for practical calculations.

The translational invariance of the system is such that the averaged quantum operators are represented in the relative coordinate form (Roth 1980):

$$\langle \boldsymbol{r}|M(\boldsymbol{R},\boldsymbol{R}')|\boldsymbol{r}'\rangle \equiv M(\boldsymbol{r}-\boldsymbol{R},\boldsymbol{r}'-\boldsymbol{R}';\boldsymbol{R}-\boldsymbol{R}') \tag{3.1}$$

where M represents any one of the quantum operators appearing in our equations. In accordance with (3.1) it is convenient to introduce the following Fourier transformation:

$$M_{\boldsymbol{K}}^{pp'} \equiv \int\int\int \mathrm{d}\boldsymbol{\rho}\,\mathrm{d}\boldsymbol{\rho}'\,\mathrm{d}\boldsymbol{X} \exp(\mathrm{i}\boldsymbol{K}\cdot\boldsymbol{X} - \mathrm{i}\boldsymbol{p}\cdot\boldsymbol{\rho} + \mathrm{i}\boldsymbol{p}'\cdot\boldsymbol{\rho}')\, M(\boldsymbol{\rho},\boldsymbol{\rho}';\boldsymbol{X}) \tag{3.2}$$

where $\boldsymbol{\rho} = \boldsymbol{r} - \boldsymbol{R}$, $\boldsymbol{\rho}' = \boldsymbol{r}' - \boldsymbol{R}'$ and $\boldsymbol{X} = \boldsymbol{R} - \boldsymbol{R}'$ represent the relative coordinates. The decomposition into electronic angular momentum components is then given by

$$M_{\boldsymbol{K}}^{pp'} = 4\pi \sum_{L,L'} Y_L(\boldsymbol{p}) M_{\boldsymbol{K}}^{LL'}(p,p') Y_{L'}^*(\boldsymbol{p}'). \tag{3.3}$$

The above decomposition (3.3) of (3.2) also applies to operators which do not depend on ionic variables. In the case of the free propagator, for example,

$$\langle \boldsymbol{r}|G_0|\boldsymbol{r}'\rangle = -(1/4\pi)\exp(\mathrm{i}\kappa|\boldsymbol{r}-\boldsymbol{r}'|)/|\boldsymbol{r}-\boldsymbol{r}'| \equiv G_0(\boldsymbol{\rho}-\boldsymbol{\rho}'+\boldsymbol{X}) \tag{3.4}$$

where $E \equiv \kappa^2$, and therefore it becomes

$$G_{0\boldsymbol{K}}^{LL'}(p,p') = (2\pi^2/\kappa^2)\delta(p-K)G_{0\boldsymbol{K}}^{LL'}(\kappa)(2\pi^2/\kappa^2)\delta(p'-K) \tag{3.5}$$

where

$$G_{0\boldsymbol{K}}^{LL'}(\kappa) = Y_L^*(\boldsymbol{K})[4\pi/(E-\kappa^2)]Y_{L'}(\boldsymbol{K}). \tag{3.6}$$

The 'artificial' dependence of G_0 shown in (3.4) on the ionic variables has to be assumed suitably in equations (2.2) and (2.4). In (2.2), G_0 is to be understood as $G_0(\boldsymbol{R}-\boldsymbol{R}')$ (i.e. $\boldsymbol{\rho}=\boldsymbol{r}-\boldsymbol{R}$, $\boldsymbol{\rho}'=\boldsymbol{r}'-\boldsymbol{R}'$ and $\boldsymbol{X}=\boldsymbol{R}-\boldsymbol{R}'$ in equation (3.4)) to conform with $g(\boldsymbol{R}-\boldsymbol{R}')$ attached to it. In the same way G_0 in (2.4) should be interpreted as $G_0(\boldsymbol{R}_2-\boldsymbol{R})$, since it represents the propagation to the original location $\boldsymbol{R}$ from $\boldsymbol{R}_2$ in the diagonal process of the multiple scattering.

The delta functions in (3.5) show that the free-electron propagator carries the electron momentum $p=K$, which is away from the energy shell $p=\kappa$. It is very important to note that, in the non-overlapping muffin-tin potential model, it can be replaced by the 'on-shell propagator' (Lloyd 1967) (see also Ehrenreich and Schwartz 1976) defined by

$$B_{\boldsymbol{K}}^{LL'}(p,p') \equiv (2\pi^2/\kappa^2)\delta(p-\kappa)B_{\boldsymbol{K}}^{LL'}(\kappa)(2\pi^2/\kappa^2)\delta(p'-\kappa) \tag{3.7}$$

where

$$B_{\boldsymbol{K}}^{LL'}(\kappa) \equiv \sum_{L''} \frac{4\pi(K/\kappa)^{l''}}{E-K^2} C_{L'}^{LL''} Y_{L''}(\boldsymbol{K}) \tag{3.8}$$

in so far as it represents the real propagation between two scatterers in the multiple-scattering processes. In the above equation, $C_{L'}^{LL''}$ is the Gaunt number:

$$C_{L'}^{LL''} = \int \mathrm{d}\Omega\, Y_L^*(\Omega)Y_{L'}(\Omega)Y_{L''}^*(\Omega) \tag{3.9}$$

and $B_{\boldsymbol{K}}^{LL'}(\kappa)$ differs from $G_{0\boldsymbol{K}}^{LL'}(\kappa)$ only in the factor $(K/\kappa)^{l''}$. The real-space representations of (3.7) and (3.8) are given by

$$B(\boldsymbol{\rho},\boldsymbol{\rho}';\boldsymbol{X}) = 4\pi \sum_{LL'} Y_L^*(\hat{\rho})j_l(\kappa\rho)B^{LL'}(\boldsymbol{X})j_l(\kappa\rho')Y_{L'}(\rho') \tag{3.10}$$

and

$$B^{LL'}(\boldsymbol{X}) = -\mathrm{i}\kappa \sum_{L''} C_{L''}^{LL''} 4\pi\, \mathrm{i}^{l''} h_{l''}^+(\kappa X)Y_{L''}(\boldsymbol{X}) \tag{3.11}$$

where j_l and h_l^+ are the spherical Bessel and the Hankel functions, respectively. The justification of the replacement is that

(i) in the multiple-scattering series $G_0(\boldsymbol{\rho}-\boldsymbol{\rho}'+\boldsymbol{X})$ appears in between the two scatterers located at $\boldsymbol{R}$ and $\boldsymbol{R}'$ and

(ii) $G_0(\boldsymbol{\rho}-\boldsymbol{\rho}'+\boldsymbol{X})$ coincides with $B(\boldsymbol{\rho},\boldsymbol{\rho}';\boldsymbol{X})$ provided that $|\boldsymbol{\rho}-\boldsymbol{\rho}'| \leqslant |\boldsymbol{X}|$.

The above inequality is satisfied because the vectors $\boldsymbol{\rho}=\boldsymbol{r}-\boldsymbol{R}$ and $\boldsymbol{\rho}'=\boldsymbol{r}'-\boldsymbol{R}'$ are confined in each of the non-overlapping muffin-tin spheres; otherwise the scattering amplitude for this process is zero.

In the EMA the above situation manifests itself in the fact that we obtain the same scattering path operator $Q(\boldsymbol{R},\boldsymbol{R}')$, and therefore the same T-matrix, when we replace two G_0-values in equations (2.2) and (2.4) by B. This is confirmed, for example, by the expansion of $Q(\boldsymbol{R},\boldsymbol{R}')$ into the perturbation series by iteration to see that all the free

propagators are together with the radial distribution functions, which enable the relevant two scatterers to be apart from each other by more than a muffin-tin diameter. We need to rearrange some of the terms to confirm this for the G_0-values in $Q_d(\boldsymbol{R})$ (Roth 1975, Yonezawa and Watabe 1975). The argument also tells us that insufficient consideration of the short-range order would not allow the replacement of G_0 by B. So far the EMA is known to be the only theory in which we can do this.

Once G_0 is replaced by B, it is seen by iteration that $\tilde{G}$ also has the same on-shell form as B;

$$\tilde{G}_{\boldsymbol{K}}^{LL'}(p,p') = (2\pi^2/\kappa^2)\delta(p-\kappa)\tilde{G}_{\boldsymbol{K}}^{LL'}(\kappa)(2\pi^2/\kappa^2)\delta(p'-\kappa). \tag{3.12}$$

The angular momentum decompositions of equations (2.1)–(2.4) are thus written in the form

$$Q_{\boldsymbol{K}}^{LL'}(\kappa,\kappa) = Q_d^l(\kappa)\delta_{LL'} + \sum_{L_1} Q_d^l(\kappa)\tilde{G}_{\boldsymbol{K}}^{LL_1}(\kappa)Q_{\boldsymbol{K}}^{L_1L'}(\kappa,\kappa) \tag{3.13}$$

$$\tilde{G}_{\boldsymbol{K}}^{LL'}(\kappa) = \tilde{B}_{\boldsymbol{K}}^{LL'}(\kappa) + \sum_{L_1L_2}\int_{\boldsymbol{K}'} h(\boldsymbol{K}-\boldsymbol{K}')\tilde{G}_{\boldsymbol{K}'}^{LL_1}(\kappa)Q_{\boldsymbol{K}'}^{L_1L_2}(\kappa,\kappa)\tilde{G}_{\boldsymbol{K}'}^{L_2L'}(\kappa) \tag{3.14}$$

$$Q_d^l(\kappa) = \tau^l(\kappa) + \tau^l(\kappa)\eta^l(\kappa)Q_d^l(\kappa) \tag{3.15}$$

$$\eta^l(\kappa) = \sum_{L_1L_2}\int_{\boldsymbol{K}} \tilde{G}_{\boldsymbol{K}}^{LL_1}(\kappa)Q_{\boldsymbol{K}}^{L_1L_2}(\kappa,\kappa)B_{\boldsymbol{K}}^{L_2L}(\kappa) \tag{3.16}$$

where $\tau^l(\kappa) \equiv t^l(\kappa,\kappa) = -\kappa^{-1}\exp[i\delta_l(\kappa)]\sin[\delta_l(\kappa)]$, the on-shell component of the single T-matrix, and $\tilde{B}_{\boldsymbol{K}}^{LL'}(\kappa)$ is the Fourier transform of $B^{LL'}(\boldsymbol{X})g(\boldsymbol{X})$ (note that different notations are used by Asano and Yonezawa (1980) and Huisman *et al* (1981)). We have also introduced a simplified notation

$$\int_{\boldsymbol{K}} \equiv \int \frac{d\boldsymbol{k}}{(2\pi)^3}.$$

The above equations determine only the on-shell components of $Q_{\boldsymbol{K}}$ and Q_d. However, their off-shell components are easily obtained from them by using the relations

$$Q_{\boldsymbol{K}}^{LL'}(p,p') = Q_c^l(p,p')\delta_{LL'} + f_p^l(\kappa)Q_{\boldsymbol{K}}^{LL'}(\kappa,\kappa)\tilde{f}_{p'}^{l'}(\kappa) \tag{3.17}$$

and

$$Q_d^l(p,p') = Q_c^l(p,p') + f_p^l(\kappa)Q_d^l(\kappa)\tilde{f}_{p'}^{l'}(\kappa) \tag{3.18}$$

where

$$f_p^l(\kappa) \equiv t^l(p,\kappa)\tau^l(\kappa)^{-1} \tag{3.19}$$

$$\tilde{f}_p^l(\kappa) \equiv \tau^l(\kappa)^{-1}t^l(\kappa,p) \tag{3.20}$$

where

$$Q_c^l(p,p') \equiv t^l(p,p') - t^l(p,\kappa)\tau^l(\kappa)^{-1}t^l(\kappa,p'). \tag{3.21}$$

The above equations are equivalent to equations (2.2*a*)–(2.2*c*) of Huisman *et al*. It is easy to see that they are in fact general relations, derived without approximation from the multiple-scattering expansion of the total T-matrix. Thus we only need to solve the on-shell part of the EMA equations (3.13)–(3.16). Note that Q_d becomes diagonal with respect to the angular momentum indices (this is a direct consequence of the isotropy of the system; the symmetry consideration will be discussed in a forthcoming paper in detail). Note, however, that Q_d is not the diagonal part of $Q_{\boldsymbol{K}}$ with respect to L. The

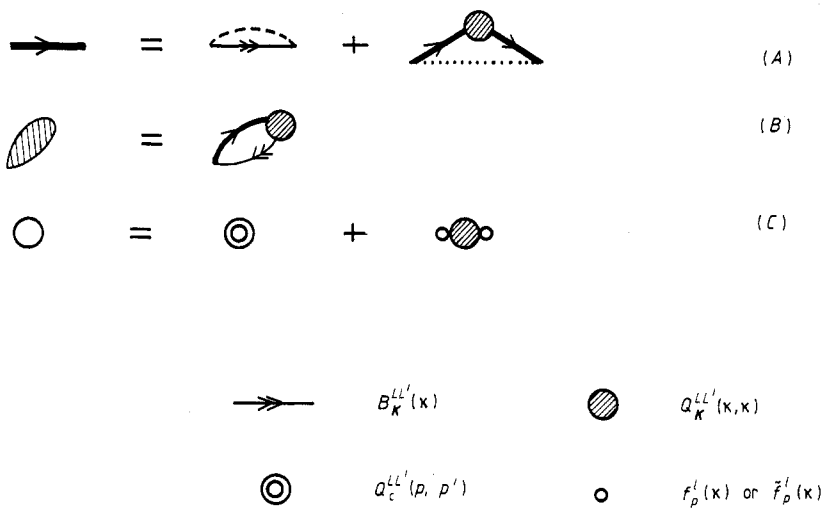

Figure 3. Separation of off-shell contributions (diagrammatic representations of equations (3.14), (3.16) and (3.17)). The off-shell corrections are expressed only by Q_c (large double circle) and f or $\tilde{f}$ (small unfilled circles).

diagrammatic representations of equations (3.14), (3.16) and (3.17) are given in figure 3 for later reference.

Next we proceed to the transport and consider the angular momentum representations of (2.10), (2.11), (2.12) and (2.14). At first sight the representation does not appear to be very useful. The argument used to reduce $\tilde{G}$ and η to the on-shell form has been dependent on the replacement of the free propagator by B and so it is not valid for $\delta\tilde{G}$ and $\delta\eta$. The replacement is not allowed for those in $\delta G_0 = G_0 J G_0'$ because they do not connect the scatterers. Nevertheless it is shown that a careful consideration of the terms leads to the classification of the contributions to the conductivity into the on-shell and the off-shell parts in a tractable way. Let us look into the diagrams in figure 2. First we note again that $\tilde{G}$ (the bold arrow in the diagram) can still be reduced to the on-shell form (3.12) in the angular momentum representation if it lies in between two scatterers. All the contributions from figures 2(A) and 2(B) are inserted in the end into figure 2(C) to calculate Ξ_c and therefore, by inspection, it is confirmed that every $\tilde{G}$ appearing in figure 2 satisfies this condition. Likewise all the G_0-values appearing in the diagrams (h)–(k) in figure 2(B) can also be replaced by B. Now suppose that we perform the iterative expansion of figures 2(A) and 2(B), and substitute all the terms obtained into figure 2(C), and that the angular momentum representation is then employed. The following expression for δG_0 can be used for this purpose:

$$\delta G_{0K}^{LL'}(p,p') = (2\pi^2/\kappa^2)\delta(p-K)\Pi_K^{LL'}(\kappa,\kappa')(2\pi^2/\kappa^2)\delta(p'-K) \tag{3.22}$$

$$\Pi_K^{LL'}(\kappa,\kappa') \equiv Y_L^*(\boldsymbol{K})[4\pi J_K/(E-K^2)(E'-K^2)]Y_{L'}(\boldsymbol{K}). \tag{3.23}$$

Because of the δ-functions in (3.7), (3.12) and (3.22) the integrations with respect to the radial parts of the internal electron momenta can now all be carried out. The contributions to Ξ_c thus obtained are then expressed in terms of the matrices $\tilde{G}_K$, B_K, Π_K and Q_K. However, there appear to be three possible forms of Q_K. The first case appears when Q lies in between the two wavy lines. The simplest examples are the terms (II) and (IV) in figure 2(C), and also (I) when figure 2(a) is substituted for $\tilde{G}$. In this case the p-integrations pick up the ionic momenta K or

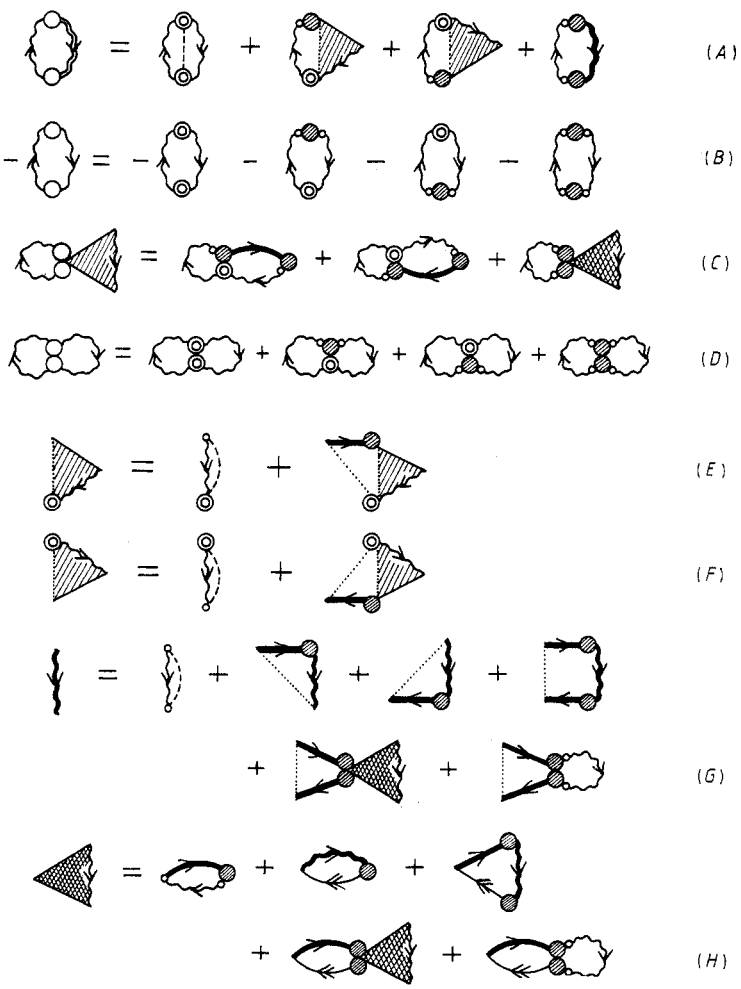

Figure 4. Reduction of the diagrammatic equations in figure 2 by using the procedure in figure 3. Note that (*G*) and (*H*) are not the equations for $\delta\tilde{G}$ and $\delta\eta$ but define the new quantities.

K' and Q takes a purely off-shell form $Q_K^{LL'}(K,K)$ or $Q_K^{LL'}(K,K')$, according to whether it is located in a closed loop (e.g. diagram (II)) or at the nodal position (e.g. diagram (IV)). In the second case, Q is situated between one wavy line and either of the two on-shell quantities B or $\tilde{G}$. In this case, Q becomes the 'half-off-shell' form $Q_K^{LL'}(K,\kappa)$ or $Q_K^{LL'}(\kappa,K)$, after p-integrations. The large circles in figures 2(*f*), 2(*g*) and 2(*k*) belong to this case. The same can be said for those in figures 2(*b*), 2(*c*), 2(*d*), 2(*h*) and 2(*i*) if figure 2(*a*) is substituted for $\tilde{G}$. The last case is when Q is not directly connected to the wavy line and the on-shell component $Q_K^{LL'}(\kappa,\kappa)$ is obtained.

The next step is to decompose Q according to figure 3(*C*). We shall therefore re-express all the diagrams in figure 2 in terms of the double circles and the large shaded circles accompanied by the small open circles. At first, it may look as if it merely introduces further complications. This procedure is not as complicated as it appears, however; the double circle survives only in between the two wavy lines,

when Q is purely off shell, since $Q_c(p, p')$ vanishes if $p = \kappa$ or $p' = \kappa$. Furthermore the small circle becomes unity when $p = \kappa$; thus it is eliminated from the diagram in that case.

The reduction of the diagrams mentioned above is completed as shown in figure 4. Note again that the wavy line is always accompanied by a double circle or a small circle at both its ends. In the latter case we treat the small circle as a part of the wavy line hereafter. The former case is a little cumbersome. A double circle $Q_c(K, K')$ at a nodal position can be neither combined with some suitable quantity nor separated from the rest of the diagram, because it contains two ionic momenta K and K'. For this reason we have introduced in figures 4(E) and 4(F) new quantities in order to represent all the contributions to $\tilde{G}$ connected to a double circle (the contributions connected to two double circles are included in the first terms of figures 4(A) and 4(D), respectively). The quantities in figures 4(G) and 4(H) form the rest of the contributions to $\delta\tilde{G}$ and $\delta\eta$, respectively, including those with small circles at either end or both ends of the diagrams according to the rule described before. We note that the second term in figure 4(C) cannot be obtained straightforwardly from figure 2(h) by the same sort of decomposition of $\delta\tilde{G}$ as that used in deriving figure 4(A). It would lead to an expression involving the quantity defined by figure 4(F). The topological equivalence between them is guaranteed by the symmetric nature of the EMA, although direct proof requires some manipulation of the diagrams.

The equations in figures 4(A)–4(H) complete the solution to our problem. It has, however, a drawback of free-electron divergence. In order to remove this, we further apply the decomposition $g = 1 + h$ to the initial terms in figures 4(A), 4(E), 4(F) and 4(G). Then the non-divergent recombinations of the terms are obtained naturally by adding figure 4(A) to 4(B), and figure 4(C) to 4(D), term by term. The result is expressed in terms of the divergence-free quantities introduced in figure 5:

$$\begin{aligned}\Xi_c(E, E') = &\int_K \int_{K'} S(\boldsymbol{K} - \boldsymbol{K}')\mathbf{Tr}[\boldsymbol{\Pi}_K Q_c(K, K')\boldsymbol{\Pi}_{K'} Q'_c(K', K)] \\ &+ \int_K \int_{K'} \mathbf{Tr}\{\boldsymbol{\Pi}_K f_K Q_K[1 + \Lambda(\boldsymbol{K}, \boldsymbol{K}')] \\ &\times (1 + \tilde{G}_{K'} Q_{K'}) = \tilde{f}'_{K'} \boldsymbol{\Pi}_{K'} Q'_c(K', K)\} \\ &+ \int_K \int_{K'} \mathbf{Tr}\{\boldsymbol{\Pi}_K Q_c(K, K')\boldsymbol{\Pi}_{K'} f'_{K'}(1 + Q'_{K'}\tilde{G}'_{K'}) \\ &\times [1 + \Lambda'(\boldsymbol{K}', \boldsymbol{K})]Q'_K \tilde{f}_K\} + \int_K \mathbf{Tr}\{\boldsymbol{\Pi}_K f_K Q_K[\boldsymbol{W}_K(\kappa, \kappa') \\ &+ \boldsymbol{K}_d(\kappa, \kappa')]Q'_K \tilde{f}'_K\} \end{aligned} \tag{3.24}$$

where $S(\boldsymbol{K}) \equiv 1 + h(\boldsymbol{K})$ is the structure factor and the argument κ has been omitted for simplicity for the on-shell quantities, i.e. $Q_K \equiv Q_K(\kappa, \kappa)$, $\tilde{G}_K \equiv \tilde{G}_K(\kappa)$, etc. The symbol **Tr** refers to the trace operation with respect to the angular momentum indices. The integral equation for $\Lambda(\boldsymbol{K}, \boldsymbol{K}')$ is obtained from figure 5(D), and those for $\boldsymbol{W}_K(\kappa, \kappa')$ and $\boldsymbol{K}_d(\kappa, \kappa')$ are derived by comparing figures 4(G) and 4(H) with figures 5(A) and 5(B):

$$\Lambda(\boldsymbol{K}, \boldsymbol{K}') = h(\boldsymbol{K} - \boldsymbol{K}') + \int_{K''} h(\boldsymbol{K} - \boldsymbol{K}'')\tilde{G}_{K''} Q_{K''} \Lambda(\boldsymbol{K}'', \boldsymbol{K}') \tag{3.25}$$

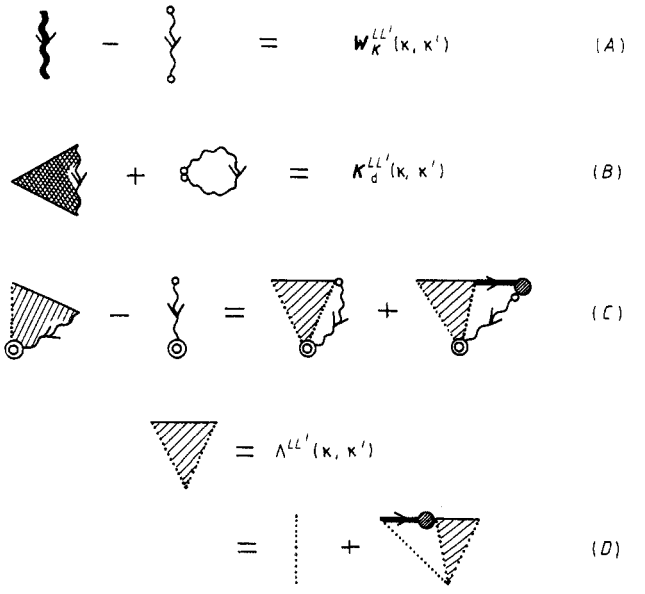

Figure 5. Definition of the divergence-free quantities.

$$\boldsymbol{W}_K = \boldsymbol{W}_{0K} + \int_{K'} h(\boldsymbol{K}-\boldsymbol{K}')[\tilde{G}_{K'}Q_{K'}\boldsymbol{W}_{K'} + \boldsymbol{W}_{K'}Q'_{K'}\tilde{G}'_{K'} + \tilde{G}_{K'}Q_{K'}(\boldsymbol{W}_{K'}+\boldsymbol{K}_{\mathrm{d}})Q'_{K'}\tilde{G}'_{K'}] \tag{3.26}$$

and

$$\boldsymbol{K}_{\mathrm{d}} = \boldsymbol{K}_{0\mathrm{d}} + \int_K [\boldsymbol{W}_K Q'_K B'_K + \tilde{G}_K Q_K(\boldsymbol{W}_K+\boldsymbol{K}_{\mathrm{d}})Q'_K B'_K] \tag{3.27}$$

where the inhomogeneous terms $\boldsymbol{W}_{0K}$ and $\boldsymbol{K}_{0\mathrm{d}}$ are given by

$$\boldsymbol{W}_{0K} = \int_K h(\boldsymbol{K}-\boldsymbol{K}')(1+\tilde{G}_{K'}Q_{K'})\tilde{f}_{K'}\boldsymbol{\Pi}_{K'}f'_{K'}(1+Q'_{K'}\tilde{G}'_{K'}) \tag{3.28}$$

and

$$\boldsymbol{K}_{0\mathrm{d}} = \int_K (1+\tilde{G}_K Q_K)\tilde{f}_K\boldsymbol{\Pi}_K f_K(1+Q'_K B'_K). \tag{3.29}$$

The above result (equations (3.24)–(3.29)) is free of divergence. Although the free-electron divergences at $K=\kappa$ appear in $\boldsymbol{\Pi}_K$, $\tilde{G}_K$ and B_K, they are suppressed by $Q_{\mathrm{c}}(K,K')$, Q_K, $1+Q_K\tilde{G}_K$ and $1+Q_K B_K$.

In order to obtain the conductivity, we must solve equations (3.25)–(3.27) simultaneously. Their solutions are then substituted into (3.24). Note that equations (3.25)–(3.27) are written solely in terms of the on-shell quantities except for f_K and $\tilde{f}_K$ included in the inhomogeneous terms. The evaluation of the off-shell corrections are thus almost separated from the main part of the calculation.

Some complication due to the off-shell problem still remains. First we must perform the double integrations in the first three lines of (3.24). Secondly the equation for $\Lambda(\boldsymbol{K},\boldsymbol{K}')$ is laborious to solve compared with (3.26) and (3.27). By putting $Q_{\mathrm{c}}=0$ we

are released from the above complications and the labour involved is reduced to the level of the tight-binding calculation performed by Itoh and Watabe (1984). In this connection it is remarkable that our equations (3.26) and (3.27), together with the last term of (3.24), have recovered the original mathematical structure; notwithstanding we still preserve the major part of the off-shell corrections by keeping f_K and $\tilde{f}'_K$ in the last term of (3.24) and in (3.28) and (3.29). In fact our numerical test using the square well potential showed that $Q_c(K, K')$ is very small compared with τ, which represents the typical magnitude of the on-shell component of Q_K. Even at the maximum position it is 100 times smaller than τ. The maximum positions are of course far from the energy shells $K = \kappa$ or $K' = \kappa$, where $Q_c(K, K')$ is zero. Therefore, as the peak position of the spectral density is around the energy shell, the contributions to Ξ_c from the double integrals in (3.24) are expected to be extremely small. We thus conclude that Q_c can be neglected for practical purposes and the off-shell corrections are taken into account sufficiently well through f_K and $\tilde{f}_K$.

4. Summary and discussion

One of the most important features in the transport problem in liquid and amorphous metals is that the influence of the atomic short-range order is crucial. The fact is obvious if we recall that the structure factor has a drastic effect in applying the Ziman formula for resistivity. The same effect is expected to be even more enhanced for non-simple materials in which the potential scattering is strong; a slight change in atomic positions should make a substantial difference in the scattering processes if the potential is strong (in this connection we note that the distinction must be made between the scattering due to the potential and that due to the disorder in discussing the transport processes).

It is well known that the EMA is the most reliable theoretical scheme in the above respect. Its application to transport in the muffin-tin potential model is expected to be fruitful considering its success in electronic structure calculations. We have shown that the 'horrendous' equations for the vertex corrections are simplified and written in a divergence-free form, keeping the off-shell contributions. The resulting equations are very similar in structure to those in the electronic structure calculations. We have thus solved the most difficult part of the problem and derived the necessary equations for discussing electron transport. Mathematical treatment of the integral equations is not as easy as in the electronic structure calculations because of the vector nature of the relevant quantities. This will be discussed in the forthcoming paper.

Acknowledgment

The authors would like to express their gratitude to the Swiss National Foundation for financial support.

References

Asano S and Yonezawa F 1980 *J. Phys. F: Met. Phys.* **10** 75
Ehrenreich H and Schwartz L 1976 *Solid State Phys.* **31** 149 (New York: Academic)
Evans R, Greenwood D A and Lloyd P 1971 *Phys. Lett.* A **35** 57
Huisman L, Nicholson D, Schwartz L and Bansil A 1981 *Phys. Rev.* B **24** 1824

Itoh M, Niizeki K and Watabe M 1981 *J. Phys. F: Met. Phys.* **11** 1605
Itoh M and Watabe M 1984 *J. Phys. F: Met. Phys.* **14** 1847
Lloyd P 1967 *Proc. Phys. Soc.* **90** 207, 217
Nishikawa A and Niizeki K 1984 *J. Non-Cryst. Solids* **62** 1331
Roth L 1975 *Phys. Rev.* B **11** 3769
—— 1980 *Phys. Rev.* B **22** 2793
Roth L and Singh V 1982 *Phys. Rev.* B **25** 2522
Watabe M and Yonezawa F 1975 *Phys. Rev.* B **11** 4753
Yonezawa F, Roth L and Watabe M 1975 *J. Phys. F: Met. Phys.* **5** 435
Yonezawa F and Watabe M 1975 *Phys. Rev.* B **11** 4746